

# Magnetic characterization of the upper pseudogap phase in cuprates

Zheng-Cheng Gu and Zheng-Yu Weng

Center for Advanced Study, Tsinghua University, Beijing 100084, China

(Received 6 June 2005; published 30 September 2005)

It is proposed that the *upper* pseudogap phase (UPP) observed in the high- $T_c$  cuprates correspond to the formation of spin singlet pairing under the bosonic resonating-valence-bond (RVB) description. We present a series of evidence in support of such a scenario based on the calculated magnetic properties including uniform spin susceptibility, spin-lattice relaxation and spin-echo decay rates, which consistently show that strong spin correlations start to develop upon entering the UPP, being *enhanced* around the momentum  $(\pi, \pi)$  while *suppressed* around  $(0, 0)$ . The phase diagram in the parameter space of doping concentration, temperature, and external magnetic field is obtained based on the the bosonic RVB theory. In particular, the competition between the Zeeman splitting and singlet pairing determines a simple relation between the “critical” magnetic field,  $H_{PG}$ , and characteristic temperature scale,  $T_0$ , of the UPP. We also discuss the magnetic behavior in the *lower* pseudogap phase at a temperature  $T_b$  lower than  $T_0$ , which is characterized by the formation of Cooper pair amplitude where the low-lying spin fluctuations get suppressed at both  $(0, 0)$  and  $(\pi, \pi)$ . Properties of the UPP involving charge channels will be also briefly discussed.

DOI: [10.1103/PhysRevB.72.104520](https://doi.org/10.1103/PhysRevB.72.104520)

PACS number(s): 74.20.Mn, 74.72.-h, 75.10.Jm, 76.60.-k

## I. INTRODUCTION

The pseudogap phase has been widely regarded as an essential integral part of the cuprate superconductors with extensive experimental support.<sup>1</sup> The underlying physics of such a phase has been a central focus in the study of high- $T_c$  problem for many years, and yet no consensus has been reached concerning its nature due to the very complexity of pseudogap phenomena observed in magnetic, transport, single-particle, and optical channels. More and more experimental evidence in recent years further indicates the existence of two kinds of pseudogap regimes at different temperatures.<sup>1–6</sup>

Among various theoretical proposals for the pseudogap phase, the resonating-valence-bond (RVB) idea<sup>7</sup> is uniquely interesting, which actually “predicted”<sup>7–10</sup> the existence of a pseudogap state in doped Mott insulators before experiment. In the RVB picture, neutral spins form the singlet pairs that are condensed as a spin liquid. The density of states of spin excitations for such a system generally gets suppressed at low energy, exhibiting a pseudogap feature as it costs energy to break up the RVB pairs to create spin excitations. In such a scenario, there is usually no gap in the pure charge degrees of freedom, and the pseudogap phenomena observed in the charge transport, angle-resolved photoemission spectroscopy (ARPES), and tunneling experiments are all indirectly attributed to the appearance of the *spin* gap in the spin degrees of freedom.<sup>9</sup> For instance, in the charge transport the strong scattering between the charge carriers and low-lying spin fluctuations becomes weakened because of the reduction of the latter in the pseudogap regime. The pseudogap feature exhibited in the ARPES and tunneling measurements may be also interpreted as due to the opening of a pseudogap associated with the spin degrees of freedom.

However, the original RVB description, known as the fermionic RVB (f-RVB) since it involves the pairing of *fermionic* “spinons” (neutral  $S=1/2$  object),<sup>9</sup> also suffers some notable inconsistency with the experiment. Note that the

pseudogap phenomenon has been found in the underdoped regime of the cuprates<sup>1</sup> where the antiferromagnetic (AF) correlations are usually quite strong. But in an f-RVB description, the AF correlations remain intrinsically weak, even at half-filling, where the AF long range order (AFLRO) develops in the cuprates at low temperature. Here the key issue is not about whether one can construct an AFLRO in the RVB background, which may be easy to incorporate by a simple mean-field order parameter.<sup>11,12</sup> But the crucial and highly nontrivial issue is whether the *whole* low-lying AF spin correlations are intrinsically and sufficiently strong in an RVB state,<sup>13</sup> and whether they are capable of continuously *growing* with reducing temperature or doping as has been clearly manifested experimentally in, say, the NMR spin-lattice relaxation rates (see the analysis in Refs. 14–18).

Since the pseudogap phase, which involves high-energy or temperature and short distance physics, may be properly considered as an unstable fixed point state<sup>10</sup> with intrinsic instabilities towards AFLRO or *d*-wave superconductivity at low temperatures, the importance of its correct description, with regard to the latter, is like that of a Fermi liquid with regard to the BCS superconducting state. In other words, finding an accurate and correct description of the pseudogap phase will be rather important for constructing a sensible low-energy theory for describing the low-temperature AF and superconducting phases in the cuprates.

In this paper, we show that there does exist a desirable candidate for characterizing the pseudogap phase based on the RVB picture, in which strong AF correlations are present as an *intrinsic* and *predominant* feature. Such an RVB state, known as the bosonic RVB (b-RVB) state,<sup>19</sup> differs from the usual f-RVB states in that it works very well at half-filling in describing the AF correlations over a wide range of temperature, including zero temperature where an AFLRO naturally emerges. Figure 1 schematically illustrates the global phase diagram for such a b-RVB theory,<sup>20</sup> where an *upper* pseudogap phase (UPP) below the characteristic temperature  $T_0$  is characterized by the formation of singlet pairing of

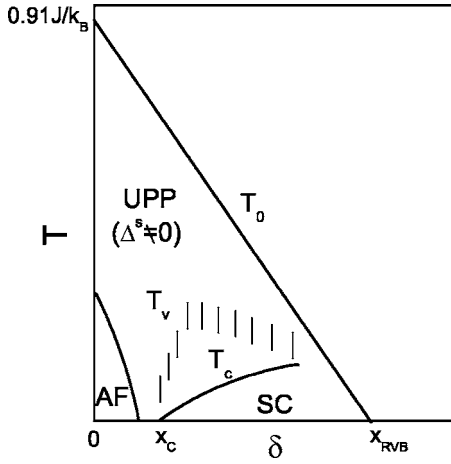


FIG. 1. The global phase diagram in the b-RVB description (Ref. 20). The upper pseudogap phase (UPP) is characterized by the bosonic RVB pairing order parameter  $\Delta^s$  at  $T \leq T_0$  whose properties are the main focus of this paper. The antiferromagnetic ordered phase (AF), the lower pseudogap phase at  $T \leq T_v$ , and the superconducting phase (SC) at  $T \leq T_c$  all happen on top of this UPP at low doping.

neutral spins as denoted by the b-RVB order parameter  $\Delta^s$ . As illustrated by Fig. 1, the low-temperature phases, including a *lower* pseudogap phase below  $T_v$  (also known as the spontaneous vortex phase),<sup>21</sup> a *d*-wave superconducting phase at  $T_c < T_v$  beyond a critical doping concentration  $x_c$ , and an AFLRO phase near half-filling, can all be regarded as the results of the low-temperature instabilities from such an UPP.<sup>20</sup>

The main focus of the present work will be the nature of the UPP itself. We will examine the detailed behavior of uniform spin susceptibility, spin-lattice relaxation rates, and spin-echo decay rate based on the b-RVB theory, which will reveal that, as one enters the UPP from above  $T_0$ , the spin correlations change qualitatively. At the mean-field level, localized spins are essentially uncorrelated at  $T > T_0$ , resulting in a Curie-Weiss-like behavior in the uniform spin susceptibility. Below  $T_0$ , however, finite-range spin correlations start to develop, predominantly around the AF momentum  $\mathbf{Q}_{AF} = (\pi, \pi)$ , with the weight being transferred from the momentum  $\mathbf{Q}_0 = (0, 0)$ . The latter effect leads to the reduction of uniform susceptibility at  $T < T_0$ . We show that such magnetic behavior in the UPP is quite consistent with the experimental measurements in the cuprates.

The above results clearly indicate that the UPP corresponds to a crossover from a weakly correlated localized spin system at higher temperature into a strongly AF correlated spin liquid at lower temperature. This picture is thus in sharp contrast to the f-RVB picture of the pseudogap, where the low-energy spin excitations, either around  $\mathbf{Q}_{AF}$  or  $\mathbf{Q}_0$ , all get suppressed with the opening of the pseudogap. This latter behavior rather resembles the lower pseudogap phase of the b-RVB theory at  $T \leq T_v$  (in Ref. 22 it is simply called the pseudogap phase) than the UPP. But even the distinction between the pseudogap state of the f-RVB theory and such a lower pseudogap state of the b-RVB theory is very significant as has been discussed in Ref. 22: the former is exchange

energy driven while the latter is kinetic energy driven. Here the lower pseudogap phase corresponds to the formation of Cooper pair amplitude but is short of superconducting phase coherence, which exists between  $T_v$  and  $T_c$  and can be regarded as a vortex liquid state.<sup>21</sup> It was previously pointed out in Ref. 21 that such a spontaneous vortex phase should coincide with the experimentally discovered Nernst region<sup>23</sup> in the high- $T_c$  cuprates.

The quantitative phase diagram of the UPP is determined in the three-dimensional parameter space of temperature, doping concentration, and external magnetic field. The latter introduces the competition between the Zeeman spin splitting and singlet spin pairing. The mean-field theory will predict a simple proportional relation between the “critical” magnetic field  $H_{PG}$ , at which the UPP is destroyed, and  $T_0$  in zero field. A comparison with experiment will be made.

The remainder of the paper is arranged as follows. In Sec. II A, the bosonic RVB description is briefly reviewed. In Sec. II B, the definition of the upper pseudogap phase is given and its phase diagram is determined. In Secs. II C and II D, its magnetic properties are systematically investigated in the framework of the b-RVB theory. In Sec. II E, we further briefly discuss the lower pseudogap phase and related magnetic behavior. Finally, Sec. III is devoted to conclusion and discussion, where we also briefly discuss the qualitative behavior of charge channels in the pseudogap phase within the bosonic RVB description.

## II. UPPER PSEUDOGAP PHASE IN THE BOSONIC RVB THEORY

### A. Bosonic RVB description

The so-called b-RVB state<sup>20</sup> is underpinned by a *bosonic RVB order parameter*  $\Delta_{ij}^s$  over a wide range of temperature and doping as schematically shown in Fig. 1, which defines the UPP. This UPP (before the emergence of low-temperature AF and superconducting instabilities) will be the main subject to be examined in the present work. In the following we shall first discuss its “mean-field” description based on the *t*-*J* model.

In the phase string representation<sup>24</sup> of the *t*-*J* model (see Appendix A), a natural “mean-field” decoupling of the superexchange term  $H_J$  is given as follows:<sup>19</sup>

$$H_J \rightarrow H_s = -\frac{J}{2} \sum_{\langle ij \rangle \sigma} \Delta_{ij}^s e^{i\sigma A_{ij}^h} b_{i\sigma}^\dagger b_{j-\sigma}^\dagger + \text{H.c.} + \text{const.}, \quad (1)$$

where the b-RVB order parameter  $\Delta_{ij}^s$  is defined in terms of the bosonic spinon annihilation operator  $b_{i\sigma}$  by

$$\Delta_{ij}^s = \sum_{\sigma} \langle e^{-i\sigma A_{ij}^h} b_{i\sigma} b_{j-\sigma} \rangle. \quad (2)$$

At half-filling,  $\Delta_{ij}^s$  is equivalent to the usual Schwinger-boson mean-field order parameter as  $A_{ij}^h = 0$ , with Eq. (1) reducing to the Schwinger-boson mean-field Hamiltonian<sup>25</sup> which describes the AF correlations fairly well in the regime of  $\Delta_{ij}^s \neq 0$  at  $T < T_0 = 0.91 J/k_B$ . Away from half-filling, a topological link field  $A_{ij}^h$  emerges in the Hamiltonian (1) as well as in Eq. (2), which represents the influence of the nonlocal phase

string effect induced by the hole hopping<sup>24</sup> on the spin degrees of freedom. It is related to the hole density by the following gauge invariant relation:<sup>24</sup>

$$\sum_{(ij) \in C} A_{ij}^h = \pi \sum_{l \in \Sigma_C} n_l^h, \quad (3)$$

where  $C$  denotes an arbitrary loop on the square lattice that encloses a region  $\Sigma_C$ , and  $n_l^h$  is the holon number operator at site  $l$ .

The “mean-field” Hamiltonian (1) is by nature a gauge model, which is invariant under the  $U(1)$  transformation:  $b_{i\sigma} \rightarrow b_{i\sigma} e^{i\sigma\theta_i}$  and  $A_{ij}^h \rightarrow A_{ij}^h + (\theta_i - \theta_j)$ . It can be easily shown that the spin rotational symmetry is respected by Eq. (1) by verifying  $[H_s, \mathbf{S}] = 0$  where the definition of the spin operator  $\mathbf{S}$  in the phase string representation is given in Appendix A. In the low-temperature regime, where the *bosonic* holons in the b-RVB theory will experience the Bose condensation such that one may approximately treat  $A_{ij}^h$  as describing a uniform flux of the strength  $\delta\pi$  per plaquette ( $\delta$  denotes the doping concentration of holes).<sup>19</sup> In the high-temperature regime,  $A_{ij}^h$  may be treated as describing randomly distributed static  $\pi$  flux tubes of concentration  $\delta$  since the holons will behave like incoherent objects there.<sup>22</sup> Different from a usual Jordan-Wigner phase, the gauge field  $A_{ij}^h$ , which is seen by spinons, is attached to an *independent* degree of freedom, holons, and therefore the above approximations are reasonable.

In both limits, the bilinear form of Eq. (1) in terms of the bosonic spinon operator  $b_{i\sigma}$  can be diagonalized by the following Bogoliubov transformation:<sup>19</sup>

$$b_{i\sigma} = \sum_m [u_{m\sigma}(i) \gamma_{m\sigma} - v_{m\sigma}(i) \gamma_{m-\sigma}^\dagger], \quad (4)$$

with

$$\begin{aligned} u_{m\sigma}(i) &= u_m w_{m\sigma}(i) \\ v_{m\sigma}(i) &= v_m w_{m\sigma}(i), \end{aligned} \quad (5)$$

where  $w_{m\sigma}(i)$  satisfies the following eigenequation:

$$\xi_m w_{m\sigma}(i) = -\frac{J}{2} \sum_{j=nn(i)} \Delta_{ij}^s e^{-i\sigma A_{ji}^h} w_{m\sigma}(j), \quad (6)$$

in which  $j=nn(i)$  denotes the four nearest neighbors ( $nn$ ) of site  $i$ . One has  $u_m = (1/\sqrt{2})\sqrt{(\lambda/E_m)+1}$  and  $v_m = \text{sgn}(\xi_m) \times (1/\sqrt{2})\sqrt{(\lambda/E_m)-1}$ , where  $E_m = \sqrt{\lambda^2 - \xi_m^2}$  is the spinon spectrum. The Lagrangian multiplier  $\lambda$  is determined by enforcing the average constraint  $\langle \sum_{\sigma} b_{i\sigma}^\dagger b_{i\sigma} \rangle = 1 - \delta$ , which leads to

$$2 - \delta = \frac{1}{N} \sum_m \frac{\lambda}{E_m} \coth \frac{\beta E_m}{2} \quad (7)$$

$$\sum_{(ij)} |\Delta_{ij}^s|^2 = \sum_m \frac{\xi_m^2}{J E_m} \coth \frac{\beta E_m}{2}, \quad (8)$$

where  $\beta = 1/k_B T$  and the last equation is obtained by the self-consistent condition (2) for the RVB order parameter. Note that a Bose condensed term  $n_{BC}^b$  related to the AFLRO

(Ref. 19) at  $T=0$  and half-filling has been dropped in Eq. (13) since we shall mainly be interested in the high-temperature behavior.

All the nontrivial effect of doping is reflected in the eigen equation (6) where the phase string effect induced by hopping enters via the topological gauge field  $A_{ij}^h$ . Note that the spinon wave function  $w_{m\sigma}(i)$  should vanish at the hole sites (where  $\Delta_{ij}^s=0$ ) due to the no-double-occupancy condition. Previously,<sup>19</sup> such an equation has been solved by a simple mean-field choice  $\Delta_{ij}^s[j=nn(i)] = \Delta^s$  with the relaxed constraint condition such that the spinons can go to any sites. In the following we still relax the no-double-occupancy constraint on average in Eq. (6), but with a replacement of

$$J \rightarrow J_{\text{eff}} = (1 - 2g\delta)J \quad (9)$$

to represent the average effect of the reduction of the super-exchange coupling around holes: if holes are static, each of which will simply break two  $nn$  links in each direction such that  $g=1$  in the dilute hole limit (when the average hole-hole distance is much larger than the  $nn$  links). Generally  $g>1$  for a moving hole since the suppression of  $\Delta_{ij}^s$  around each hole extends more than the four broken  $nn$  bonds (e.g., from the singular twist by  $A_{ij}^h$  around each hole). One may thus approximately rewrite Eq. (6) as

$$\xi_m w_{m\sigma}(i) = -J_s \sum_{j=nn(i)} e^{-i\sigma A_{ji}^h} w_{m\sigma}(j), \quad (10)$$

in which

$$J_s \equiv \frac{J_{\text{eff}} \Delta^s}{2},$$

and Eq. (8) can be consistently rewritten as

$$\Delta^s = \frac{1}{4N} \sum_m \frac{\xi_m^2}{J_s E_m} \coth \frac{\beta E_m}{2}. \quad (11)$$

Note that the same mean-field equations have been obtained in Ref. 19 with a slightly different definition, i.e., with  $\Delta^s$  replaced by  $\Delta^s/(1-2g\delta) = \Delta_1^s$  (with  $g=1$ ) in Ref. 19.

### B. Upper pseudogap phase

The UPP is defined by the formation of the b-RVB pairing with  $\Delta^s \neq 0$ . Its high-temperature boundary at  $\Delta^s=0$  is depicted by a characteristic temperature  $T_0$  as illustrated in Fig. 1. In the following, we determine it based on the mean-field theory outlined above.

According to Eq. (7), one finds

$$2 - \delta = \coth \frac{\lambda}{2k_B T_0} \quad (12)$$

by noting that  $\xi_m \rightarrow 0$  at  $\Delta^s \rightarrow 0$ . Consequently, Eq. (11) reduces to  $1 = (2 - \delta)(1/2N) \sum_m (\xi_m/\Delta^s)^2 / J_{\text{eff}} \lambda$ , which gives rise to

$$\lambda = \frac{2 - \delta}{2} J_{\text{eff}} \quad (13)$$

by further identifying

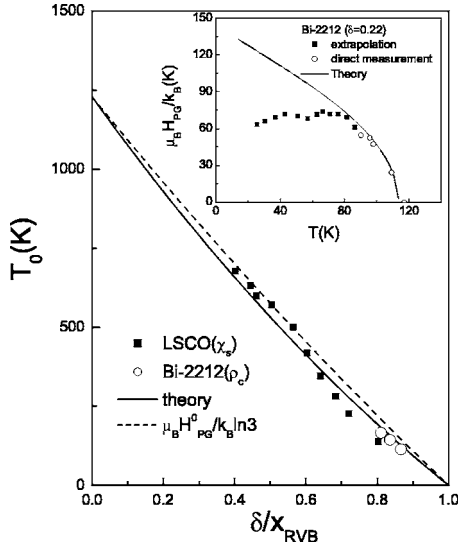


FIG. 2. The characteristic temperature  $T_0$  of the UPP versus  $\delta/x_{\text{RVB}}$ . Solid line: the present theory; Full squares: determined from the uniform spin susceptibility  $\chi_s$  in LSCO compound (Ref. 27); Open circles: determined from the  $c$  axis magnetoresistivity ( $\rho_c$ ) measurement in Bi-2212 compound (Ref. 28); The dashed line shows the scaling relation of the zero-temperature critical field  $H_{\text{PG}}^0$  with  $T_0$  as predicted by the theory. Inset: the critical field  $H_{\text{PG}}$  as a function of temperature at  $\delta=0.22$ . The experiment data from the  $c$  axis transport in Bi-2212 (Ref. 28) are also shown by the open and full squares.

$$\frac{1}{N} \sum_m (\xi_m / \Delta^s)^2 = J_{\text{eff}}^2 \quad (14)$$

in terms of Eq. (10). Finally one obtains

$$k_B T_0 = \left( \frac{1 - \frac{\delta}{2}}{\ln \frac{3 - \delta}{1 - \delta}} \right) J_{\text{eff}}. \quad (15)$$

It is interesting to note that the gauge field  $A_{ij}^h$  does not explicitly appear in  $T_0$  because of the general relation (14), indicating that the phase string effect, which is crucial to the low-temperature (low-energy) physics, actually plays no role in determining the phase boundary of the UPP. Of course, the hopping effect still enters in  $T_0$  via the renormalized factor  $g$  in  $J_{\text{eff}}$  which shall be the only adjustable parameter depending on the detailed physics of local hopping. We find that the phase diagram and magnetic properties to be studied below are actually not sensitive to  $g$  except for the characteristic concentration  $x_{\text{RVB}}$  at which  $J_{\text{eff}}$  is extrapolated to zero at  $T=0$ .

Figure 2 shows  $T_0$  (solid curve) as a function of  $\delta/x_{\text{RVB}}$  with  $J=1350$  K. The experimental data determined by the uniform spin susceptibility measurement in LSCO (Refs. 26 and 27) (see the discussion in the next section) are shown by the full squares, which are in good agreement with the theoretical curve. Furthermore, the open circles are independently determined from the  $c$ -axis transport<sup>28</sup> in the over-

doped regime (see discussion below). Note that the theoretical curve  $T_0$  versus  $\delta/x_{\text{RVB}}$  in Fig. 2 is not sensitive to the choice of  $g$ . Furthermore, one can use the above experimental data<sup>26–28</sup> to fix  $x_{\text{RVB}}$  at  $x_{\text{RVB}}=1/2g=0.25$  ( $g=2$ ). We shall then choose  $x_{\text{RVB}}=0.25$  throughout the rest of paper without any more adjustable parameter.

For the b-RVB origin of the UPP, the Zeeman splitting due to the external magnetic field can effectively destroy the singlet pairing of spins in the strong field limit. Since the orbit part of the neutral spins does not couple to the external field directly, the Zeeman splitting will be the only direct field effect on the RVB background. It thus provides a direct probe of the RVB nature of the UPP in, say, the overdoped regime, where the critical field strength may be within the experimental accessible range. In the following we consider the Zeeman effect in the UPP.

Apply an external magnetic field  $\mathbf{H}$  along a spin  $z$  axis (which is not necessarily perpendicular to the lattice plane). A spin Zeeman energy term should be then added to  $H_s$  in Eq. (1),

$$-2\mu_B \sum_i S_i^z H = -\mu_B H \sum_{\sigma} \sigma \gamma_{m\sigma}^{\dagger} \gamma_{m\sigma}. \quad (16)$$

Consequently the spinon excitation spectrum is modified by

$$E_m^{\sigma} = E_m - \sigma \mu_B H, \quad (17)$$

which now explicitly depends on the spin index  $\sigma$ . Then the mean-field Eq. (12) at  $\Delta^s \rightarrow 0$  is modified to

$$2 - \delta = \frac{1}{2} \sum_{\sigma} \coth \frac{E^{\sigma}}{2T k_B}, \quad (18)$$

with  $E^{\sigma} \equiv \lambda - \sigma \mu_B H$ , while Eq. (13) remains the same. From these equations, we can easily obtain the following relation between  $T_0$  at zero field and the zero-temperature “critical” field  $H_{\text{PG}}^0$  at which  $\Delta^s$  vanishes,

$$\mu_B H_{\text{PG}}^0 = \ln \left( \frac{3 - \delta}{1 - \delta} \right) k_B T_0, \quad (19)$$

with the coefficient only weakly dependent on the doping concentration. In Fig. 2,  $\mu_B H_{\text{PG}}^0 / k_B \ln 3$  is plotted as the dashed curve which scales with the zero-field  $T_0$  fairly well, which predicts

$$\mu_B H_{\text{PG}}^0 \approx 1.1 k_B T_0. \quad (20)$$

In general, the temperature dependence of the “critical” field  $H_{\text{PG}}(T)$  can be obtained based on Eqs. (18) and (13). In the inset of Fig. 2,  $H_{\text{PG}}$  versus  $T$  at  $\delta=0.22$  is shown together with the experimental data obtained from the  $c$ -axis magneto transport measurements.<sup>28</sup> We see that the *high-temperature* experimental data (open circles) fit the theoretical curve very well without any additional adjustable parameter. Furthermore the zero-field  $T_0$  determined by the *same* experiments is also in good agreement with the theory as shown (open circles) in the main panel of Fig. 2 as mentioned above. One may also note that the experimental  $H_{\text{PG}}(T)$  starts to deviate from the theoretical curve in the inset (full squares) as the temperature is further lowered and saturated to approximately half of the predicted number (which implies  $\mu_B H_{\text{PG}}^0$



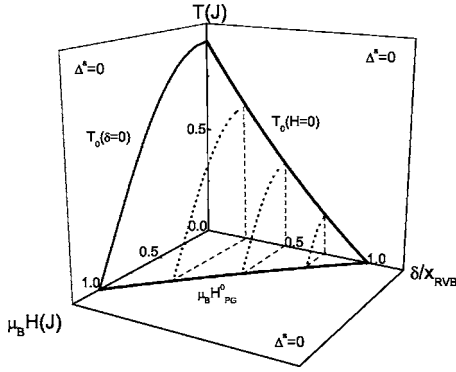


FIG. 3. The phase diagram of the UPP in the parameter space of doping, temperature, and external magnetic field, as calculated based on the mean-field bosonic RVB theory.

$\simeq k_B T_0/2$ ). However, we would like to point out that such a deviation occurs only for those data (full squares) which have been obtained by *extrapolation* in the experimental measurement<sup>28</sup> and therefore may not be as reliable as the higher temperature ones (open squares) in the inset of Fig. 2. We believe that further experiments are needed in order to convincingly verify (falsify) the present prediction (20).

Finally the boundaries of the UPP in the three-dimensional parameter space of doping concentration, temperature, and magnetic field determined based on the b-RVB mean-field theory are shown in Fig. 3.

### C. Uniform spin susceptibility

The RVB nature of the UPP is clearly manifested in the magnetic properties. We first consider uniform spin susceptibility  $\chi_s$  in the following, which can be easily derived based on the above mean-field description in the presence of magnetic field. In terms of the total spin magnetic moment,

$$M = \mu_B \sum_m [n(E_m^+) - n(E_m^-)], \quad (21)$$

[where  $n(\omega) = 1/(e^{\beta\omega} - 1)$  is the Bose distribution function], the uniform spin susceptibility  $\chi_s$  per site as defined by  $\chi_s = M/NH|_{H \rightarrow 0}$  is found by

$$\chi_s = \frac{2\mu_B^2\beta}{N} \sum_m n(E_m)[1 + n(E_m)]. \quad (22)$$

Since we are mainly interested in the high-temperature regime well above the superconducting phase, the holes are incoherent objects such that  $A_{ij}^h$  can be approximately treated as describing randomly distributed  $\pi$  flux tubes of concentration  $\delta$  as discussed before. Then we can numerically calculate  $\chi_s$  based on the mean-field equations given in Sec. II A, which is averaged under different random configurations of  $A_{ij}^h$ . A similar computation has been done before to explore the crossover from the lower to upper pseudogap phases,<sup>22</sup> but not in the region up close to  $T_0$ . (In the following calculations, the largest sample size is  $32 \times 32$  lattice and the sample size is not very important as mainly the high-temperature properties are concerned.)

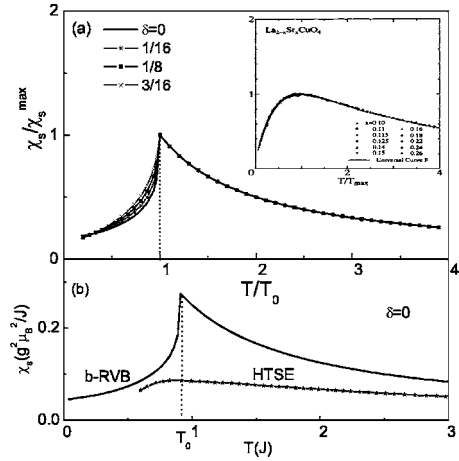


FIG. 4. (a) The calculated uniform spin susceptibility  $\chi_s$  scaled with the maximum  $\chi_s^{\max}$  at  $T_0$  versus  $T/T_0$ , which follows an approximately doping-dependent curve. Inset: The experimental data in Refs. 26 and 27 which collapse into a universal scaling curve plotted in the same fashion as in the main panel. (b) The theoretical  $\chi_s$  at half-filling (solid) and the one obtained by the high-temperature series expansion (HTSE). The latter fits the experimental scaling curve in the inset of (a) very well (Refs. 26 and 27).

The calculated  $\chi_s$  is presented in the main panel of Fig. 4(a) at different doping concentrations. Note that  $\chi_s$  reaches a maximum value  $\chi_s^{\max}$  at temperature  $T_0$  where the RVB order parameter  $\Delta^s$  vanishes. At  $T > T_0$ ,  $\chi_s$  follows a Curie- $1/T$  behavior as spins become free moments at the mean-field level. The curves in Fig. 4(a) are presented as  $\chi_s/\chi_s^{\max}$  versus  $T/T_0$ , which approximately collapse onto a single curve independent of doping. For comparison, the inset shows the experimental data obtained in LSCO compounds which are plotted in the same way as in the main panel with a very good collapsing onto a universal scaling curve.<sup>26,27</sup> The peak positions decides the experimental pseudogap temperature  $T_0$ 's at different dopings, which are presented in Fig. 2.

In Fig. 4(b), the calculated  $\chi_s$  versus  $T$  at  $\delta=0$  is shown together with the high-temperature series expansion (HTSE) result.<sup>29</sup> (Note that here the calculated  $\chi_s$  is rescaled by a  $2/3$  numerical factor as used in the Schwinger-boson approach to restore the sum rule.<sup>25</sup>) It is noted that the experimental scaling curve actually coincides with the half-filling HTSE very well.<sup>26,27</sup> Thus one can clearly see the overall qualitative agreement between the bosonic RVB theory and the experiment from Figs. 4(a) and 4(b). Note that the mean-field  $\chi_s$  deviates from the HTSE result prominently around  $T_0$  where the latter is a much smoother function of  $T$ . It reflects the fact that  $T_0$  is only a crossover temperature and the vanishing  $\Delta^s$  does not represent a true phase transition. Obviously, the amplitude fluctuations beyond the mean-field  $\Delta^s$  have to be considered in order to better describe  $\chi_s$  in this regime.  $T_0$  determined in the mean-field theory is quite close to the HTSE result, indicating the crossover temperature itself can still be reasonably decided by the mean-field bosonic RVB description given above. The comparison of  $T_0$  between the theory and experiment has been already presented in Fig. 2 and discussed in the previous section.

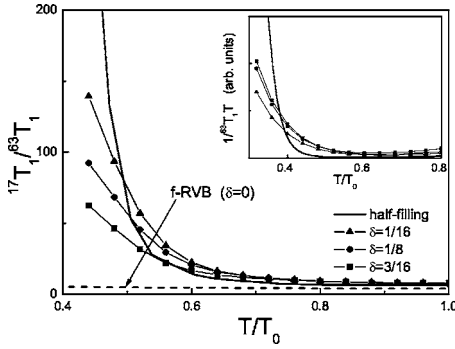


FIG. 5.  $^{17}T_1/^{63}T_1$  vs temperature at different doping concentrations in the upper pseudogap phase of the b-RVB state. The dashed line shows the result of an f-RVB state ( $\pi$  flux phase) at half-filling. The inset shows the non-Korringa behavior of  $1/^{63}T_1T$  in the b-RVB state at various dopings (the symbols are the same as in the main panel).

#### D. Spin-lattice relaxation rate and spin-echo decay rate

The NMR spin-lattice relaxation rate of nuclear spins is determined by<sup>30</sup>

$$\frac{1}{T_1} = \frac{2k_B T}{g^2 \mu_B^2 N} \sum_{\mathbf{q}} F(\mathbf{q})^2 \left. \frac{\chi''_{zz}(\mathbf{q}, \omega)}{\omega} \right|_{\omega \rightarrow 0^+}, \quad (23)$$

where the form factor  $F(\mathbf{q})^2$  comes from the hyperfine coupling between nuclear spin and spin fluctuations. For example, for planar  $^{63}\text{Cu}(2)$  nuclear spins in the cuprates, with the applied field perpendicular to the  $\text{CuO}_2$  plane, the form factor  $F(\mathbf{q})^2$  is found to be<sup>15,16</sup>

$$^{63}F(\mathbf{q})^2 = [A_{\perp} + 2B(\cos q_x a + \cos q_y a)]^2, \quad (24)$$

where the hyperfine couplings  $A_{\perp}$  and  $B$  are estimated as  $A_{\perp}/B \approx 0.84$ ,  $B \approx 3.8 \times 10^{-4}$  meV.<sup>16</sup> (These coefficients may slightly vary among YBCO and LSCO compounds.) For planar  $^{17}\text{O}(2)$  nuclear spins, one has

$$^{17}F(\mathbf{q})^2 = 2C^2 \left[ 1 + \frac{1}{2}(\cos q_x a + \cos q_y a) \right], \quad (25)$$

with  $C \approx 0.87B$ . Due to the fact that  $^{17}F(\mathbf{q})^2$  vanishes at the AF wave vector  $\mathbf{Q}_{\text{AF}} = (\pi, \pi)$ , while  $^{63}F(\mathbf{q})^2$  is peaked at  $\mathbf{Q}_{\text{AF}}$ , a combined measurement of  $1/^{63}T_1$  and  $1/^{17}T_1$  will thus provide important information about the AF correlations at low frequency  $\omega \rightarrow 0$ .

Based on the bosonic RVB mean-field equations outlined in Sec. II A, the spin-lattice relaxation rates,  $1/^{63}T_1$  and  $1/^{17}T_1$ , for the planar copper and oxygen nuclear spins, can be straightforwardly computed as shown in Appendix B. The results are presented in Fig. 5. It shows that the ratio  $^{17}T_1/^{63}T_1$ , which is a constant above  $T_0$ , starts to increase with reducing temperature below  $T_0$ . At lower temperature,  $T/T_0 < 0.5$ , such a ratio rises sharply. For example,  $^{17}T_1/^{63}T_1$  diverges at  $\delta=0$  as a true AFLRO exists at  $T=0$ , and it still reaches about 100 in the low-temperature limit at  $\delta=0.125$ , all qualitatively consistent with the experimental observation in the cuprates.<sup>17</sup> As pointed out above, such behavior clearly demonstrates that strong low-lying AF correlations around  $\mathbf{Q}_{\text{AF}}$  develop in the UPP, leading to the simultaneous en-

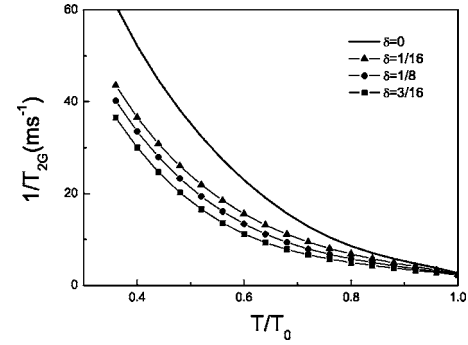


FIG. 6.  $1/T_{2G}$  vs temperature in the upper pseudogap phase below  $T_0$  at different doping concentrations.

hancement of  $1/^{63}T_1$  and the cancellation in  $1/^{17}T_1$ . In the inset of Fig. 5,  $1/^{63}T_1T$  has been plotted, which is also qualitatively consistent with the experiment,<sup>16–18</sup> but deviates from the conventional Korringa behavior  $1/^{63}T_1T \sim \text{const}$  for a Fermi liquid system, thanks to the strong AF fluctuations of spins in the UPP below  $T_0$ .<sup>31</sup> By contrast, the ratio  $^{17}T_1/^{63}T_1$  in an f-RVB mean-field state (the  $\pi$  flux phase) at half-filling remains flat over the whole temperature region as shown by the dashed line in Fig. 5, indicating the absence of any significant AF correlations around  $\mathbf{Q}_{\text{AF}}$  in its pseudogap regime. In combination with the reduced uniform spin susceptibility,<sup>22</sup> one sees that in the pseudogap of the f-RVB, the low-energy spin excitations, either around  $\mathbf{Q}_{\text{AF}}$  or  $\mathbf{Q}_0 = (0,0)$ , all get suppressed with the opening of the pseudogap.

The above results clearly show that the UPP in the bosonic RVB state corresponds to the crossover from a weakly correlated localized spin assembly at higher temperature into a strongly AF correlated spin liquid at lower temperature. The peculiar feature of the bosonic RVB description is that although the formation of bosonic RVB singlet pairing suppresses the spin correlations at  $\mathbf{Q}_0$  below  $T_0$ , it also leads to the *enhancement* of the low-energy spin correlations near AF momentum  $\mathbf{Q}_{\text{AF}}$ . Such a feature of the UPP is significantly different from the pseudogap phase in the f-RVB mean-field description, but is strongly supported by the NMR measurements.<sup>14–18</sup>

Finally, we further examine the spin-echo decay rate  $1/T_{2G}$ , which is related to the static AF correlations via the real part of spin susceptibility function by<sup>32</sup>

$$\left( \frac{1}{T_{2G}} \right)^2 = \frac{0.69}{8\hbar^2 (\hbar\gamma_e)^4} \left\{ \frac{1}{N} \sum_{\mathbf{q}} F_{\text{eff}}(\mathbf{q})^4 \chi'_{zz}(\mathbf{q})^2 - \left[ \frac{1}{N} \sum_{\mathbf{q}} F_{\text{eff}}(\mathbf{q})^2 \chi'_{zz}(\mathbf{q}) \right]^2 \right\}, \quad (26)$$

where the factor  $F_{\text{eff}}(\mathbf{q})$  is

$$F_{\text{eff}}(\mathbf{q}) = A_{\parallel} + 2B(\cos q_x a + \cos q_y a), \quad (27)$$

with  $A_{\parallel} \approx -4B$ , such that  $F_{\text{eff}}(\mathbf{q})$  is peaked at  $\mathbf{Q}_{\text{AF}}$  and vanish at  $\mathbf{Q}_0$ .

Similar to  $1/T_1$ , the detailed expression of  $1/T_{2G}$  in the bosonic RVB theory is given in Appendix C. In Fig. 6, the

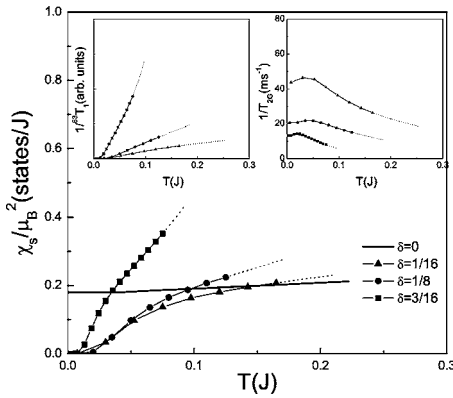


FIG. 7. Uniform spin susceptibility in the *lower* pseudogap phase at different dopings including half-filling. The left inset shows  $1/T_1$  and the right inset  $1/T_{2G}$  with the same symbols as in the main panel.

calculated  $1/T_{2G}$  at different doping concentrations show that  $1/T_{2G}$  begins to increase with reducing temperature below  $T_0$ . Such behavior has been also observed in the experiment,<sup>33–35</sup> which once again clearly illustrates the picture that the strong AF correlations start to develop in the UPP.

### E. Lower pseudogap phase

So far we have been focused on the UPP, which is the high-temperature phase in the bosonic RVB description. As stressed in Sec. I, there can be several different low-temperature phases growing out of this background (Fig. 1).<sup>20</sup> One particular phase we wish to discuss below is the so-called spontaneous vortex phase<sup>21</sup> which can be properly classified as the lower pseudogap phase in the present approach. In this phase, the holon condensation occurs and Cooper pair amplitude forms, but the system is still short of superconducting phase coherence which can be regarded as a vortex liquid state due to the presence of unpaired spinon-vortex composites.<sup>21</sup> These spinon-vortices contribute to the Nernst effect and therefore the lower pseudogap phase should coincide with the Nernst region discovered<sup>23</sup> experimentally in the cuprates. Recently the electromagnetic response of such a vortex liquid phase has been also discussed<sup>36</sup> based on a different RVB approach.

Previously the magnetic properties in this phase was discussed<sup>22</sup> in the context of exploring the driving mechanism in comparison with the pseudogap phase in the *f*-RVB state. In the following, we focus on the magnetic behavior of this lower pseudogap phase and contrast it with that of the UPP discussed above.

The mean-field equations are the same as in the UPP, but due to the holon condensation the gauge field  $A_{ij}^h$  in Eq. (10) can be treated as a uniform flux of strength  $\pi\delta$  per plaquette<sup>22</sup> as discussed in Sec. II A. In the main panel of Fig. 7, the uniform spin susceptibility shows a true “spin gap” behavior, in contrast to the “scaling” curve shown in the UPP in Fig. 4, where  $\chi_s$  in the doped regime roughly behaves like that at half-filling—in the latter case  $\chi_s$  saturates to a constant at  $T=0$ . In the lower pseudogap phase, these  $\chi_s$ ’s

can drop below that at  $\delta=0$  and vanish at  $T=0$  as shown in Fig. 7. Such a lower pseudogap behavior has been indeed observed experimentally.<sup>2,9</sup>

Furthermore, in this lower pseudogap phase,  $1/^{63}T_1$  also decreases with temperature (see the left inset of Fig. 7), as opposed to the behavior in the UPP, indicating the appearance of the spin gap over whole momenta. On the other hand, although the low-energy spin fluctuations are gapped, the static AF spin-spin correlations as described by the real part of spin susceptibility function still remain, as reflected by  $1/T_{2G}$  shown in the right inset of Fig. 7, where the monotonic increase of  $1/T_{2G}$  in the UPP (Fig. 6) is replaced by the saturation at lower pseudogap phase. This feature has also been observed experimentally.<sup>33–35</sup>

### III. CONCLUSION AND DISCUSSION

In this paper, we have systematically analyzed the magnetic characterizations of a high-temperature *intrinsic* phase of the bosonic RVB state, which is described by the formation of the bosonic RVB order parameter at a temperature below the characteristic  $T_0$ , but still higher than those for low-temperature orders, including AFLRO and superconductivity, to emerge.

Such a phase exhibits the pseudogap features that match those of the upper pseudogap phase in the high- $T_c$  cuprate superconductors very well. The key feature in the crossover to the UPP from above  $T_0$  is the onset of the development of strong AF spin-spin correlations, which remain rather weak at  $T > T_0$  where the system resembles more an ensemble of uncorrelated localized spins. This explains why experimentally the uniform spin susceptibility shows an approximately Curie-Weiss behavior at  $T > T_0$ , reaches a peak at  $T_0$ , and then gets reduced below  $T_0$  as the weight of the spin-spin correlations at the momentum  $(0,0)$  being transferred to  $(\pi, \pi)$ , in contrast to an equal weight distribution above  $T_0$ . It further explains why the spin-lattice relaxation rate gets enhanced for the planar copper nuclear spins whereas reduced for the planar oxygen nuclear spins below  $T_0$ , and why the spin-echo decay rate increases with the decreasing temperature; Clearly the development of the AF correlations is the underlying mechanism here.

We emphasize that the formation of spin singlet pairing and the onset of AF correlations at the same time are not always true. In the *f*-RVB description of the slave-boson approach, the formation of the *f*-RVB order parameter actually leads to the reduction of the spin-lattice relaxation rates for both the copper and oxygen nuclear spins at low temperatures. This is because the spin pseudogap opens for both the ferromagnetic and AF correlations. By contrast, this case occurs in the *b*-RVB description only at a lower temperature when the system enters the lower pseudogap regime, characterized by the formation of Cooper pair amplitude in the so-called spontaneous vortex phase<sup>21</sup> which is a vortex liquid state, short of superconducting phase coherence. A comparative study of this lower pseudogap phase in the *b*-RVB theory and the pseudogap phase in the *f*-RVB theory has been given in Ref. 22 where two opposite driving mechanisms, kinetic vs superexchange energy driven, have been identified.

The phase diagram of the UPP has been determined by a generalized “mean-field” description in the b-RVB theory in the parameter space of temperature, doping, and magnetic field. Since the UPP essentially reflects the spin singlet pairing, the Zeeman splitting competes directly, which results in a quantitative prediction for experiment as discussed in Sec. II B.

A central consequence of an RVB (spin singlet) description of the pseudogap phase is that the pseudogap represents the suppression of the low-lying spectral weight in spin excitations, but not in charge excitations, as pointed out in the Sec. I. In the following, we briefly outline the scenario about what happens to the charge channel when one enters the UPP in the bosonic RVB theory. We shall leave the more quantitative investigation in future work.

In order to see how the charge transport is affected by the spin fluctuations, we first note that in the b-RVB theory, the charge degrees of freedom (holons) are described by the following effective Hamiltonian:<sup>19</sup>

$$H_h = -t_h \sum_{\langle ij \rangle \sigma} e^{iA_{ij}^s} h_i^\dagger h_j + \text{H.c.}, \quad (28)$$

where the bosonic holons, created by  $h_i^\dagger$ , interact with the gauge field  $A_{ij}^s$  associated with the spin degrees of freedom. Similar to the definition of the gauge field  $A_{ij}^h$  in Eq. (3),  $A_{ij}^s$ , which is introduced in the phase string representation (see Appendix A), satisfies

$$\sum_{\langle ij \rangle \in C} A_{ij}^s = \pi \sum_{l \in \Sigma_C} (n_{l\uparrow}^b - n_{l\downarrow}^b), \quad (29)$$

where  $C$  is an arbitrary path. Physically  $A_{ij}^s$  describes  $\pm\pi$  flux tubes bound to  $\uparrow(\downarrow)$  spinons as seen by holons. So at  $T > T_0$ , uncorrelated localized spins imply a maximum scattering to the holons according to Eqs. (28) and (29). By forming the RVB pairing below  $T_0$ , one can easily understand that the fluctuations in  $A_{ij}^s$  will be effectively reduced, and so does the scattering to the holons according to Eqs. (28) and (29), leading to a pseudogap feature in the charge transport without involving a charge gap. Note that when the temperature is further reduced to  $T_v$ , where the holons gain the phase coherence and become Bose condensed, the system enters the lower pseudogap phase (spontaneous vortex phase) in which the effect of the holon condensation will feed back to the spinon part via  $A_{ij}^h$  in Eq. (1) and cause the lower pseudogap phenomenon in the spin part as discussed in Sec. II E. Finally, the quasiparticle excitation can be regarded as a recombination of holon, spinon, and phase string, in the superconducting phase.<sup>37</sup> It has been argued that the deconfinement occurs above  $T_c$ , and the composite structure is expected to show up in both the lower and upper pseudogap phases, and the pseudogap feature is thus believed to be associated with that in the spinon degrees of freedom.

#### ACKNOWLEDGMENTS

We are grateful for helpful discussions with V. N. Muthukumar, T. Senthil, D. N. Sheng, and H. H. Wen. The authors also acknowledge support from NSFC and MOE grants. This

research was also supported in part by the NSF under Grant No. Phy99-07949 via KITP at UC Santa Barbara where this work was completed.

#### APPENDIX A: PHASE STRING FORMULATION

The  $t$ - $J$  model

$$H_{t-J} = -t \sum_{\langle ij \rangle \sigma} (c_{i\sigma}^\dagger c_{j\sigma} + \text{H.c.}) + J \sum_{\langle ij \rangle} \left( \vec{S}_i \cdot \vec{S}_j - \frac{1}{4} n_i n_j \right) \quad (A1)$$

may be reformulated by using the phase string decomposition<sup>24</sup>

$$c_{i\sigma} = (-\sigma) i h_i^\dagger b_{i\sigma} e^{i\Theta_{i\sigma}^{\text{string}}}, \quad (A2)$$

where  $h_i$  and  $b_{i\sigma}$  are all *bosonic fields*. Here  $\Theta_{i\sigma}^{\text{string}}$  is a non-local phase factor to restore the fermionic statistics of the electron operator, and can be expressed as  $\Theta_{i\sigma}^{\text{string}} \equiv \frac{1}{2} [\Phi_i^b - \sigma \Phi_i^h]$  with  $\Phi_i^b = \sum_{l \neq i} \theta_l(l) (\sum_{\alpha} \alpha n_{l\alpha}^b - 1)$ ,  $\Phi_i^h = \sum_{l \neq i} \theta_l(l) n_l^h$ . Here  $\theta_l(l)$  is defined as an angle  $\theta_l(l) = \text{Im} \ln(z_i - z_l)$  with  $z_i = x_i + iy_i$  representing the complex coordinate of a lattice site  $i$ . The resulting Hamiltonian  $H_{t-J} = H_t + H_J$  reads

$$H_t = -t \sum_{\langle ij \rangle \sigma} (e^{i(A_{ij}^s - \phi_{ij}^0)} h_i^\dagger h_j (e^{i\sigma A_{ij}^h} b_{j\sigma}^\dagger b_{i\sigma} + \text{H.c.}))$$

$$H_J = -\frac{J}{2} \sum_{\langle ij \rangle \sigma \sigma'} (e^{i\sigma A_{ij}^h} b_{i\sigma}^\dagger b_{j-\sigma}^\dagger (e^{i\sigma' A_{ji}^h} b_{j-\sigma'} b_{i\sigma'} + \text{H.c.})) \quad (A3)$$

under the no-double-occupancy constraint

$$h_i^\dagger h_i + \sum_{\sigma} b_{i\sigma}^\dagger b_{i\sigma} = 1. \quad (A4)$$

In the new Hamiltonians,  $\phi_{ij}^0$  is a  $\pi$  flux link variable, while  $A_{ij}^s$  and  $A_{ij}^h$  are constrained by the following conditions:

$$\sum_C A_{ij}^s = \pi \sum_{l \in C} (n_{l\uparrow}^b - n_{l\downarrow}^b) \quad (A5)$$

$$\sum_C A_{ij}^h = \pi \sum_{l \in C} n_l^h, \quad (A6)$$

where  $C$  is an arbitrary counterclockwise closed path. Finally, in the phase string representation, the spin operators can be easily reexpressed according to the decomposition (A2) as

$$S_i^z = \frac{1}{2} \sum_{\sigma} \sigma b_{i\sigma}^\dagger b_{i\sigma},$$

$$S_i^\sigma = (-1)^i b_{i\sigma}^\dagger b_{i-\sigma} e^{i\sigma \Phi_i^h}. \quad (A7)$$

#### APPENDIX B: $1/T_1$ FORMULATION IN THE BOSONIC RVB REPRESENTATION

$1/T_1$  defined in Eq. (23) can be reexpressed in terms of the real-space spin correlation function as follows:



$$\frac{1}{T_1} = \frac{2k_B T}{g^2 \mu_B^2 N} \sum_{ij} M_{ij} \left. \frac{\chi''_{zz}(i, j, \omega)}{\omega} \right|_{\omega \rightarrow 0^+}, \quad (\text{B1})$$

where  $M_{ij}$  is the Fourier transformation of  $F(\mathbf{q})^2$  in real space

$${}^{63}M_{ij} \equiv (A_{\perp}^2 + 4B^2) \delta_{i,j} + 2A_{\perp} B \sum_{\hat{\eta}} \delta_{i,j+\hat{\eta}} + B^2 \sum_{\hat{\eta} \neq -\hat{\eta}'} \delta_{i,j+\hat{\eta}+\hat{\eta}'}, \quad (\text{B2})$$

where  $\hat{\eta} = \pm \hat{x}, \pm \hat{y}$ , and

$${}^{17}M_{ij} \equiv 2C^2 \left( \delta_{i,j} + \frac{1}{4} \sum_{\hat{\eta}} \delta_{i,j+\hat{\eta}} \right). \quad (\text{B3})$$

From  $M_{ij}$  we see that only up to the next-nearest-neighbor spin correlations are involved in the spin-lattice relaxation rates of  ${}^{63}\text{Cu}$  and  ${}^{17}\text{O}$  nuclear spins.

In the bosonic RVB mean-field theory, by using Eq. (4) the dynamic spin susceptibility can be expressed as

$$\left. \frac{\chi''_{zz}(i, j, \omega)}{\omega} \right|_{\omega \rightarrow 0^+} = G_{ij}^- + (-1)^{i-j} G_{ij}^+, \quad (\text{B4})$$

where

$$G_{ij}^{\pm} = \frac{\pi}{2} \sum_{mm'}' K_{mm'}^{zz}(i, j) \left( -\frac{\partial n(E_m)}{\partial E_m} \right) (p_{mm'}^{\pm})^2 \delta(E_m - E_{m'}), \quad (\text{B5})$$

in which  $\Sigma'$  denotes the summation of  $m$  with  $\xi_m > 0$  and

$$K_{mm'}^{zz}(i, j) \equiv \sum_{\sigma} w_{m\sigma}^*(i) w_{m\sigma}(j) w_{m'\sigma}^*(j) w_{m'\sigma}(i). \quad (\text{B6})$$

By noting that  $p_{mm'}^- = 1$ ,  $p_{mm'}^+ = \lambda/E_m$  at  $E_m = E_{m'}$ , we can further reexpress  $1/T_1$  in the following form:

$$\frac{1}{T_1} = \frac{2}{3g^2 \mu_B^2 N} \sum_m' n(E_m) [1 + n(E_m)] \rho(E_m) \left[ D_m^- + \frac{\lambda^2}{E_m^2} D_m^+ \right], \quad (\text{B7})$$

where the density of states  $\rho(E_m) = (2/N) \sum_m' \delta(E_m - E_{m'})$  and the coefficient,  $D_m^{\pm}$ , is defined by

$$D_m^{\pm} = \frac{\sum_m' d_{mm'}^{\pm} \delta(E_m - E_{m'})}{\sum_m' \delta(E_m - E_{m'})}, \quad (\text{B8})$$

with

$$d_{mm'}^{\pm} \equiv \frac{\pi}{2} N \sum_{ij} K_{mm'}^{zz}(i, j) (\mp)^{i-j} M_{ij}. \quad (\text{B9})$$

In Eq. (B7) a numerical factor 2/3 is also added just like the uniform spin susceptibility as noted in the main text as at half-filling.<sup>25</sup> The final result will be an average over different random configurations of  $A_{ij}^h$  due to the incoherent distribution of holes in the UPP. (In the lower pseudogap phase, by contrast, the holon condensation leads to a uniform flux distribution of  $A_{ij}^h$  and no such average is needed.) The calculation is done on a  $32 \times 32$  lattice and results are presented in Fig. 5.<sup>31</sup>

### APPENDIX C: SPIN-ECHO RELAXATION RATE

The spin-echo relaxation rate  $1/T_{2G}$  is defined in Eq. (26). In the b-RVB theory, the real part of the static susceptibility,  $\chi'_{zz}(\mathbf{q})$ , can be expressed as

$$\chi'_{zz}(\mathbf{q}) = \chi'^+_{zz}(\mathbf{q}) + \chi'^-_{zz}(\mathbf{q}), \quad (\text{C1})$$

with

$$\chi'^{\pm}_{zz}(\mathbf{q}) = \frac{2}{3} \times \frac{1}{2} \sum_{mm'}' K_{mm'}^{zz}(\mathbf{q}) \left[ (p_{mm'}^{\pm})^2 \frac{[n(E_{m'}) - n(E_m)]}{E_m - E_{m'}} + (l_{mm'}^{\pm})^2 \frac{[1 + n(E_m) + n(E_{m'})]}{E_m + E_{m'}} \right], \quad (\text{C2})$$

where

$$p_{mm'}^{\pm} = u_m u_{m'} \pm v_m v_{m'},$$

$$l_{mm'}^{\pm} = u_m v_{m'} \pm v_m u_{m'} \quad (\text{C3})$$

and

$$K_{mm'}^{zz}(\mathbf{q}) \equiv \frac{1}{N} \sum_{ij\sigma} e^{i\mathbf{q} \cdot (\mathbf{r}_i - \mathbf{r}_j)} w_{m\sigma}^*(i) w_{m\sigma}(j) w_{m'\sigma}^*(j) w_{m'\sigma}(i). \quad (\text{C4})$$

The numerical calculation is similar to that for  $1/T_1$ .

<sup>1</sup>For a review, see, T. Timusk and B. Statt, Rep. Prog. Phys. **62**, 61 (1999).

<sup>2</sup>K. Ishida, K. Yoshida, T. Mito, Y. Tokunaga, Y. Kitaoka, K. Asayama, A. Nakayama, J. Shimoyama, and K. Kishio, Phys. Rev. B **58**, R5960 (1998).

<sup>3</sup>T. Watanabe, T. Fujii, and A. Matsuda, Phys. Rev. Lett. **84**, 5848 (2000).

<sup>4</sup>R. S. Markiewicz, Phys. Rev. Lett. **89**, 229703 (2002).

<sup>5</sup>T. Timusk, Solid State Commun. **127**, 337 (2003).

<sup>6</sup>Y. Ando, S. Komiya, K. Segawa, S. Ono, and Y. Kurita, Phys. Rev. Lett. **93**, 267001 (2004).

<sup>7</sup>P. W. Anderson, Science **235**, 1196 (1987).

<sup>8</sup>G. Kotliar and J. Liu, Phys. Rev. B **38**, R5142 (1988). For a review, see, P. A. Lee, N. Nagaosa, and X.-G. Wen, cond-mat/0410445 (unpublished).

<sup>10</sup>P. W. Anderson, cond-mat/0108522 (unpublished); P. W. Anderson, cond-mat/0201431 (unpublished).

<sup>11</sup>T. C. Hsu, Phys. Rev. B **41**, 11379 (1990).

- <sup>12</sup>Chang-Ming Ho, V. N. Muthukumar, Masao Ogata, and P. W. Anderson, Phys. Rev. Lett. **86**, 1626 (2001).
- <sup>13</sup>Some enhancement of antiferromagnetic correlations in the f-RVB theory by including gauge field fluctuations has been discussed in W. Rantner and X. G. Wen, Phys. Rev. B **66**, 144501 (2002).
- <sup>14</sup>F. Mila and T. M. Rice, Phys. Rev. B **40**, R11382 (1989).
- <sup>15</sup>B. S. Shastry, Phys. Rev. Lett. **63**, 1288 (1989).
- <sup>16</sup>A. J. Millis, H. Monien, and D. Pines, Phys. Rev. B **42**, 167 (1990).
- <sup>17</sup>M. Takigawa, A. P. Reyes, P. C. Hammel, J. D. Thompson, R. H. Heffner, Z. Fisk, and K. C. Ott, Phys. Rev. B **43**, 247 (1991).
- <sup>18</sup>T. Imai, C. P. Slichter, K. Yoshimura, and K. Kosuge, Phys. Rev. Lett. **70**, 1002 (1993).
- <sup>19</sup>Z. Y. Weng, D. N. Sheng, and C. S. Ting, Phys. Rev. Lett. **80**, 5401 (1998); Phys. Rev. B **59**, 8943 (1999).
- <sup>20</sup>Z. Y. Weng, in *Proceedings of the International Symposium on Frontiers of Science*, Beijing 2002 (World Scientific, 2003); cond-mat/0304261 (unpublished).
- <sup>21</sup>Z. Y. Weng and V. N. Muthukumar, Phys. Rev. B **66**, 094509 (2002).
- <sup>22</sup>Z. C. Gu, T. Li, and Z. Y. Weng, Phys. Rev. B **71**, 064502 (2005).
- <sup>23</sup>Y. Wang, S. Ono, Y. Onose, G. Gu, Y. Ando, Y. Tokura, S. Uchida, and N. Ong, Science **299**, 86 (2003); Y. Wang, Z. A. Xu, T. Kakeshita, S. Uchida, S. Ono, Y. Ando, and N. P. Ong, Phys. Rev. B **64**, 224519 (2001); Z. A. Xu, N. P. Ong, Y. Wang, T. Kakeshita, and S. Uchida, Nature (London) **406**, 486 (2000).
- <sup>24</sup>Z. Y. Weng, D. N. Sheng, Y.-C. Chen, and C. S. Ting, Phys. Rev. B **55**, 3894 (1997).
- <sup>25</sup>A. Auerbach and D. P. Arovas, Phys. Rev. Lett. **61**, 617 (1988).
- <sup>26</sup>D. C. Johnston, Phys. Rev. Lett. **62**, 957 (1989).
- <sup>27</sup>T. Nakano, M. Oda, C. Manabe, N. Momono, Y. Miura, and M. Ido, Phys. Rev. B **49**, 16000 (1994).
- <sup>28</sup>T. Shibauchi, L. Krusin-Elbaum, M. Li, M. P. Maley, and P. H. Kes, Phys. Rev. Lett. **86**, 5763 (2001); L. Krusin-Elbaum, T. Shibauchi, and C. H. Mielke, *ibid.* **92**, 097005 (2004).
- <sup>29</sup>G. S. Rushbrooke and P. J. Wood, Mol. Phys. **1**, 257 (1958); M. E. Lines, Phys. Rev. **164**, 736 (1967); L. J. de Jongh and A. R. Miedema, Adv. Phys. **23**, 1 (1974).
- <sup>30</sup>T. Moriya, Prog. Theor. Phys. **28**, 371 (1962).
- <sup>31</sup>Note that in the inset of Fig. 5,  $1/^{63}\text{Tl}T$  is shown only below  $T \leq 0.8T_0$ , as  $1/^{63}\text{Tl}T$  is ill defined at  $T_0$  in the mean-field description where  $\Delta^s=0$ . Such an ill behavior is also reflected in the uniform susceptibility in Fig. 2 by a sharp cusp at  $T_0$  as compared to the broad, smooth peak in the HTSE result and experimental data. This is due to the fact that there is no true phase transition at  $T_0$  and the description beyond the mean-field order parameter  $\Delta^s$  is needed in order to more accurately describe the crossover behavior in the transition regime. On the other hand, the ratio  $^{17}\text{Tl}/^{63}\text{Tl}$  still remains well defined around  $T_0$  in the mean-field state as shown in the main panel of Fig. 5.
- <sup>32</sup>D. Thelen and D. Pines, Phys. Rev. B **49**, 3528 (1994).
- <sup>33</sup>M. Takigawa, Phys. Rev. B **49**, 4158 (1994).
- <sup>34</sup>R. L. Corey, N. J. Curro, K. O'Hara, T. Imai, C. P. Slichter, K. Yoshimura, M. Katoh, and K. Kosuge, Phys. Rev. B **53**, 5907 (1996).
- <sup>35</sup>R. Stern, M. Mali, J. Roos, and D. Brinkmann, Phys. Rev. B **51**, 15478 (1995).
- <sup>36</sup>P. W. Anderson, cond-mat/0504453 (unpublished).
- <sup>37</sup>Z. Y. Weng, D. N. Sheng, and C. S. Ting, Phys. Rev. B **61**, 12328 (2000); Y. Zhou, V. N. Muthukumar, and Z. Y. Weng, *ibid.* **67**, 064512 (2003).